Differential Immunomodulatory Properties of Langya and Nipah Virus Proteins

Stéphanie DURAND[§], Dimitrios MAROUSIS[§], Branka HORVAT*, and Louis-Marie BLOYET*

Centre International de Recherche en Infectiologie, Inserm U1111, CNRS UMR5308, Université de Lyon, Université Claude Bernard Lyon 1, École Normale Supérieure de Lyon, Lyon, France

§ Contributed equally

* Corresponding authors: branka.horvat@inserm.fr; louis-marie.bloyet@cnrs.fr

Differential Immunomodulatory Properties of Langya and Nipah Virus Proteins

ABSTRACT

Langya virus (LayV) is a shrew-borne emerging parahenipavirus first identified in 2018 in 35 febrile patients in China. The closely related Nipah virus (NiV) is a highly pathogenic emerging bat-borne henipavirus that has caused numerous outbreaks with public health concerns in Asia. Among other symptoms, NiV causes severe acute respiratory syndrome and encephalitis, leading to high lethality. Thus, although closely related, infections with these two emerging and zoonotic viruses have distinct pathogenicity. Since the interplay with the host's immune system is a key determinant of species barrier crossing and pathogenicity, we aimed at deciphering the ability of LayV to counteract the human intrinsic immunity using the better-characterised NiV as a prototype. NiV expresses the P, V, and W proteins, known to hinder the host's innate immune response during infection. We thus compared the immunomodulatory properties of LayV and NiV proteins in human cells and showed that, similarly to NiV, the C-terminal domain of LayV V proteins inhibits the response to the activation of the pattern recognition receptor MDA5. However, although the N-terminal region of LayV P can inhibit the interferon signalling, it is not as efficient as its NiV counterpart. Moreover, only NiV W inhibits MDA5 and RIG-I signalling pathways. Similarly, unlike NiV, LayV W cannot efficiently block the activation of the NF-κB promoter after stimulation with IL-1β. These results suggest that LayV is less efficient than NiV in counteracting the human intrinsic immunity, which may contribute to the difference in severity observed between NiV and LayV-infected patients.

IMPORTANCE

Langya virus (LayV) is a shrew-borne emerging parahenipavirus recently identified in patients in China with symptoms such as fever, fatigue, cough, anorexia, headache, and vomiting. Since the interaction between a virus and its host's immune system is an essential parameter influencing host adaptation and disease severity, we investigated the interplay between LayV and the human intrinsic immunity using as a prototype the better-characterized and closely related Nipah virus (NiV), a highly pathogenic henipavirus. We compared the immunomodulatory properties of LayV and NiV proteins in human cells and showed that, similarly to NiV, some of LayV proteins can inhibit human signalling pathways, while, unlike NiV, LayV W protein is unable to block essential immune pathways. This suggests that LayV is less efficient than NiV in counteracting the human intrinsic immunity, which may contribute to the difference in severity between NiV and LayV-infected patients.

KEYWORDS: Langya virus, Nipah virus, zoonosis, innate immunity, interferon, NF-κB

55 **INTRODUCTION**

56 Langya and Nipah viruses are closely related zoonotic paramyxoviruses responsible for
57 outbreaks in Asia. Langya virus (LayV) was first identified in 2018 in 35 patients with acute
58 infections in China's Henan and Shandong provinces [1]. Symptoms included fever, fatigue,
59 cough, anorexia, myalgia, nausea, headache, and vomiting. Shrews are likely the natural
60 reservoir of LayV, although seropositivity has also been detected in dogs and goats. LayV has
61 also been recently identified in shrews in the Republic of Korea [2], and closely related viruses
62 have been discovered in shrews and rodents in Asia, Africa, Europe, and North America [3–
63 10]. Due to its phylogenetic proximity with Nipah and Hendra viruses, LayV was initially
64 described as a henipavirus, but the discovery of several related shrew-borne viruses led to the
65 creation of the new *Parahenipavirus* genus [11] (Figure 1A). The ability of LayV to infect
66 humans, the severity of the symptoms, the seropositivity of domestic animals, and its
67 widespread geographic area raise concerns about its zoonotic potential. To date, no reverse
68 genetic system for LayV is available, only the structures of LayV glycoproteins have been
69 studied [12–17], and the interplay between LayV and its hosts remains unexplored.

70 Nipah virus (NiV) is a closely related emerging and highly pathogenic virus responsible
71 for regular zoonotic outbreaks in Asia [18]. Discovered during an outbreak in Malaysia in 1998,
72 NiV causes severe symptoms, including severe acute respiratory syndrome and encephalitis,
73 with a case-fatality rate ranging from 40% to 75%. Since 2001, almost annual outbreaks in
74 Bangladesh and India have been caused by spillovers from NiV natural reservoir: *Pteropus* fruit
75 bats. In the absence of approved vaccines and treatments, and reports of human-to-human
76 transmission, the World Health Organisation placed NiV on its Blueprint list of priority
77 pathogens requiring urgent research and development efforts [19].

78 NiV and LayV share a similar genome organisation with the conserved six adjacent
79 genes (Figure 1B) [2]. Most henipavirus P genes encode four proteins: P, V, W, and C proteins

80 [20]. V and W proteins are expressed from mRNAs edited by the viral polymerase during
81 transcription with the addition of one (V) or two (W) guanosine residues at a specific editing
82 site. Thus, the P, V, and W proteins share a common N-terminal domain (P_{NTD}) but differ in
83 their unique C-terminal domains (CTD) (Figure 1B). Although there is no direct evidence for
84 the existence of LayV V and W proteins, the conservation of the editing site and the sequences
85 of the V and W CTDs strongly suggests these proteins are produced during the infection (Figure
86 S1B-D).

87 NiV is well known to interfere with the host's intrinsic immunity, notably by inhibiting
88 the interferon type I (IFN-I) induction and signalling pathways, contributing to its high
89 pathogenicity [21–26]. Indeed, P_{NTD}, common to P, V, and W, binds and inhibits STAT1, thus
90 preventing the expression of interferon-stimulated genes (ISGs) [27–31,26,32,33].
91 Additionally, NiV V protein binds to MDA5, disrupts its folding, and thus prevents its
92 activation and the expression of interferon beta (IFN-β) [34–36]. Via its CTD, NiV W also
93 inhibits the NF-κB pathway by preventing the accumulation of the p65 subunit in the nucleus
94 [37].

95 Although closely related, LayV and NiV have different pathogenicity and infection
96 outcomes in humans. Since the interplay between viruses and the innate immune response plays
97 a critical role in pathogenicity, to examine these differences we compared the ability of the P,
98 V, and W proteins of LayV and NiV to counteract several pathways of the intrinsic immunity
99 in human cells.

100 **MATERIALS AND METHODS**

101

102 ***Cells***

103 Human carcinoma HeLa cell line (Cat# ATCC® CCL-2™), Human Embryonic Kidney
104 HEK293T (Cat# ATCC® CRL-3216™) and Human hepatocellular carcinoma cell line Huh-
105 7.5 (kind gift from Charles Rice (Rockefeller University, New York, USA)) were grown in
106 Dulbecco's modified Eagle's medium (DMEM), high glucose, GlutaMAX™
107 (LifeTechnologies™, Cat# 61965-026) supplemented with 10% of heat-inactivated (30 min at
108 56°C) foetal calf serum (Gibco, Cat #A5256701), and 1% of Penicillin-Streptomycin solution
109 (Life Technologies™, Cat# 15140-130). All cell types were incubated at 37°C with 5% CO_2
110 and tested negative for Mycoplasma *spp*. (Lonza, Cat#LT07-318). Depending on their features,
111 the different cell lines were used in specific assays: since they have a very high transfection
112 rate, HEK293T cells were used in the IFN-I response luciferase assay to maximize the signal-
113 to-noise ratio; due to their large cytoplasm, HeLa cells were used for microscopy and, to be
114 consistent with the p65 localization assay, for the NF-κB pathway luciferase assay; and Huh7.5
115 cells were used to study RIG-I and MDA5 since they do not express RIG-I and only a low level
116 of MDA5, thus allowing us to study one sensor or the other without interference from
117 endogenous proteins [38].

118

119 ***Plasmids***

120 The plasmids expressing the Firefly luciferase under the control of the IFN-β promoter (pβ-
121 IFN-Luc [39]), the NF-κB promoter (pSGNluc, Addgene, Cat# 186705) [40], and the interferon
122 response element (pISRE-Luc, Stratagene, Cat # 219092) were used to monitor the activation
123 of the promoters. The plasmid phRL-TK expressing the Renilla luciferase under the HSV-
124 thymidine kinase promoter (Promega, Cat# E6241) was used for normalisation. The plasmids

125 pEF_c-myc-MDA5 and pEF-BOS-HA-RIG-I encode myc-tagged human MDA5 and HA-
126 tagged human RIG-I, respectively [41].
127 Plasmids coding for LayV P, V, and W (GenBank #OM101129) were cloned in
128 pcDNA3.1 and ordered from GeneScript. These proteins contain an N-terminal Flag tag,
129 separated by a GGGSG linker. Plasmids coding for NiV proteins (GenBank #AY988601) were
130 cloned with the same tag in the same backbone using InFusion-mediated recombination
131 (Takara, Cat# 638933). To express P/V/W_{NTD}, P_{CTD} was removed from the plasmids expressing
132 P. V_{CTD} and W_{CTD} were expressed as fusion proteins with a Flag-tagged mCherry protein fused
133 at their N-terminus (separated from the CTDs by a single G residue). V and W mutants were
134 generated from the plasmids encoding the non-mutated proteins using InFusion-mediated
135 recombination.
136 The open reading frames of all plasmids were sequenced by Sanger sequencing
137 (Eurofins Genomics).
138
139 ***Luciferase reporter assays***
140 For the investigation of the MDA5 and RIG-I pathways, 2×10^4 Huh-7.5 cells were seeded per
141 well in ninety-six-well plates. Each well was transfected the day after with 50 ng of pβ-IFN-
142 Luc, 20 ng of phRL-TK, 50 ng of MDA5 or RIG-I expressing plasmid, together with 80 ng of
143 plasmids expressing the viral proteins or the mCherry control, using JetOptimus reagent
144 (Ozyme, Cat# POL101000006) according to the manufacturer's recommendations.
145 Cells were transfected 24 h later with 100 ng of Poly(I:C) (Invivogen, Cat# PIC-39-05) using
146 Lipofectamine 2000 (ThermoFisher Scientific, Cat #11668027). Medium was replaced four
147 hours after stimulation with DMEM 10% FCS. Activities of the luciferases were measured 24
148 h after stimulation.

149 To investigate the IFN-I response pathway, ninety-six-well plates were coated with 50
150 µg/mL of poly-D-lysine (ThermoFisher Scientific, Cat# A3890401) for 30 min at 37°C, then
151 washed with water and dried before being seeded with 4×10^4 HEK293T cells per well. Each
152 well was transfected the day after with 12.5 ng of pISRE-Luc, 5 ng of phRL-TK, together with
153 35.4 ng of plasmids expressing the viral proteins or the mCherry control, using JetOptimus
154 reagent (Ozyme, Cat# POL101000006) according to the manufacturer's recommendations.
155 Cells were treated the day after with 1000 U/mL of IFNα-2a (ImmunoTools, Cat#11343506)
156 for 18 h before measuring the activity of the luciferases.

157 To monitor the NF-κB pathway, 2×10^4 HeLa cells per well were seeded in ninety-six-
158 well plates. Each well was transfected the day after with 12.5 ng of pSGNluc, 6.25 ng of phRL-
159 TK, together with 31.25 ng of plasmids expressing the viral proteins or the mCherry control,
160 using JetOptimus reagent (Ozyme, Cat# POL101000006) according to the manufacturer's
161 recommendations. Cells were treated 24 h later with 10 ng/µL of human IL-1β (Peprotech, Cat#
162 200-01B) for 2 h before measuring the luciferase activities.

163 For all assays, the activities of the luciferases were measured using the Dual-Glo
164 Luciferase Assay system according to the manufacturer's protocol (Promega, Cat# E2920) and
165 a microplate reader (Tristar 5, Berthold) with acquisition for 1 s. For each well, the relative
166 luciferase activity was calculated as the ratio between the Firefly and Renilla luciferase
167 activities. For each condition, experiments were performed in triplicate and repeated in four
168 separate experiments.

169

170 ***Immunofluorescence***

171 For the detection of viral proteins, $2x10^5$ HeLa cells were seeded on 12 mm glass coverslips
172 placed in a 12-well plate. Twenty-four hours later, cells were transfected with 0.5 µg of plasmid
173 and fixed 48 h after transfection with 4% paraformaldehyde. Cells were permeabilised with

174 0.1% Triton X-100 in PBS for 20 min and blocked for 30 min in PBS - 2% BSA. Staining was
175 done overnight at 4°C using mouse anti-Flag antibody (Merck, Cat# F1804) diluted in PBS –
176 0.5% BSA, followed by incubation for 1 h at room temperature with DAPI (Thermo FisherTM,
177 Cat# 62248) and Alexa Fluor 488 goat anti-mouse antibody (ThermoFisher Scientific) diluted
178 at 1.3 µg/mL in the same buffer.

179 For the detection of p65, $2x10^5$ HeLa cells were seeded on 12 mm glass coverslips
180 placed in a 12-well plate and transfected 24 h later with 2 µg of plasmid expressing NiV or
181 LayV W or W_{CTD} proteins. Twenty-four hours after transfection, cells were stimulated or not
182 with 10 ng/mL of human IL-1β (Peprotech, Cat# 200-01B) for 20 min at 37°C before being
183 washed with ice-cold PBS and fixed in 4% paraformaldehyde for 30 min on ice. Cells were
184 then permeabilised for 10 min in TBS – 0.1% Triton X-100 and blocked for 10 additional
185 minutes in TBS – 2.5% BSA. Then, cells were stained overnight at 4°C with rabbit anti-NF-κB
186 p65 (Cell Signalling, Cat#8242) and mouse anti-Flag antibody (Merck, Cat# F1804) diluted in
187 TBS– 2% FCS - 0.1% Tween. The day after, cells were incubated for 1 h at room temperature
188 with DAPI (ThermoFisher Scientific, Cat# 62248) together with Alexa Fluor 488 donkey anti-
189 rabbit (ThermoFisher Scientific, Cat# A21206) and Alexa Fluor 555 goat anti-mouse antibodies
190 (ThermoFisher Scientific, Cat# A21422) diluted at 1.3 µg/mL in the same buffer.

191 Coverslips were mounted with Fluoromount-G (SouthernBiotech, Cat# 0100-01) before
192 observation on a confocal microscope (Zeiss, LSM800Airy Scan) hosted in the PLATIM
193 microscopy facility (SFR Biosciences, Lyon, France). Images were treated using ImageJ
194 software.

195

196 ***Quantification and statistical analysis***

197 *Luciferase assay analysis*

198 All assays with statistical analysis were performed in four independent experiments, with each
199 condition tested in triplicate (three technical replicates per plate). For each well, the Firefly
200 luciferase signal was normalised by the Renilla luciferase signal. Statistical analyses were done
201 using the non-parametric Mann-Whitney test.

202 *Image quantification*

203 Fluorescence microscopy images were analysed and quantified using QuPath 0.5.1 software
204 (https://qupath.github.io/). Cells were identified using a cell detection program based on the
205 staining of the nuclei (DAPI staining). For the quantification of the NF-κB p65 signal, the
206 nuclear signal is defined as the signal present in the mask created by the DAPI staining, and the
207 cytoplasmic signal as the signal present in a 2 µm radius outside of the nucleus mask. Each
208 condition was tested in four independent experiments with three images analysed per
209 experiment, leading to a total of 150 cells analysed per condition. Statistical analysis was done
210 using the non-parametric Mann-Whitney test.

211

212 ***Phylogenetic tree***

213 The L protein sequences from Nipah virus (NC_002728), Hendra virus (NC_001906), Cedar
214 virus (NC_025351), Ghana virus (NC_025256), Yunnan bat henipavirus 1 (PQ621839),
215 Yunnan bat henipavirus 2 (PQ621840), Angavokely henipavirus (ON613535), Gamak virus
216 (MZ574407), Crocidura tanakae henipavirus 2 (PP272531), Jingmen Crocidura shantungensis
217 henipavirus 1 (OM030314), Wufeng Crocidura attenuata henipavirus 1 (OM030317),
218 Crocidura tanakae henipavirus 1 (OQ970176), Resua virus (OR713876), Wufeng Chodsigoa
219 smithii henipavirus 1 (OM030316), Chodsigoa hypsibia henipavirus (OQ236120), Camp Hill
220 virus (PQ140948), Ninorex virus (OQ438286), Denwin virus (OR713883), Crocidura olivieri
221 henipavirus 2 (PQ541139), Melian virus (OK623353), Jingmen Crocidura shantungensis
222 henipavirus 2 (PP272750), Daeryong virus (MZ574409), Crocidura olivieri henipavirus 1

223 (PQ541138), Lechcodon virus (OR713879), Wenzhou shrew henipavirus 1 (OQ715593),
224 Hasua virus (OR713881), Mojiang virus (NC_025352), and Langya virus (OM101125), were
225 used to build a multiple sequence alignment using MAFFT [42]. The phylogenetic tree was
226 calculated with the Neighbor Joining algorithm in MAFFT.

227 **RESULTS**

228

229 ***Similar intracellular localisation of NiV and LayV P and V proteins, but different***
230 ***localisation of their W proteins***

231 While NiV P and V proteins are found in the cytoplasm, W is concentrated in the nucleus
232 [29,43,44,37]. To investigate if LayV proteins harbour the same cellular localisation, we
233 transfected NiV and LayV proteins fused to a Flag tag in HeLa cells and observed their
234 localisations by immunofluorescence. Similar to NiV, LayV P and V proteins are both localised
235 in the cytoplasm (Figure 2A, B). On the contrary, NiV and LayV W proteins are found in
236 different cell compartments, with NiV W being restricted to the nucleus while LayV W is
237 diffused in the cytoplasm (Figure 2C). These results correlate with the presence of a nuclear
238 localisation signal (NLS) located on NiV W_{CTD} and the absence of conservation of these
239 residues in LayV W (Figure S1D) [45].

240

241 ***NiV and LayV P proteins inhibit the IFN-I signalling pathway***

242 Via their common N-terminal domain (P_{NTD}), NiV P, V, and W proteins inhibit the transcription
243 factor STAT1, leading to a decrease in IFN-I signalling [27–31,26,32,33]. To monitor this
244 effect, the highly transfectable HEK293T cells were transfected with plasmids encoding the
245 viral proteins and a reporter gene under the control of the Interferon-Stimulated Response
246 Element (ISRE). After stimulation with IFN-2α, the reporter signal was significantly decreased
247 for cells expressing NiV and LayV P proteins compared to the control cells expressing the
248 fluorescent protein mCherry (Figure 3A). Similarly to NiV, LayV P_{NTD} is sufficient to mediate
249 this inhibition (Figure 3B). However, although LayV P and P_{NTD} expression levels were higher
250 or similar to NiV proteins, LayV proteins were less efficient in blocking the signalling (Figure

251 3, S2A). This difference may be linked to the low conservation of the STAT1-binding region
252 identified on NiV P and thus to a lower affinity for human STAT1 (Figure S1A).
253
254 ***NiV and LayV V proteins inhibit MDA5 but not RIG-I signalling pathways***
255 The C-terminal domain of V proteins is capable of binding MDA5, disrupting its folding, and
256 inhibiting the subsequent activation of the IFN-β promoter [34–36,46]. To compare the effect
257 of NiV and LayV V proteins on the IFN-β induction pathway after MDA5 or RIG-I transfection
258 and activation, we used Huh-7.5 cells since they do not express RIG-I and only a low level of
259 MDA5 [38]. NiV and LayV V proteins are both capable of inhibiting the induction of the IFN-
260 β promoter upon MDA5 activation (Figure 4A, S2B). This effect is even stronger when only
261 the V_{CTD} is expressed as a fusion protein with mCherry (mCh-V_{CTD}) (Figure 4B, S2B). As
262 expected, a mutant of NiV V_{CTD} carrying the mutations E411A and I414A, known to impair the
263 binding to MDA5 [47], is no longer able to inhibit the activation of the IFN-β promoter (Figure
264 4B). On the contrary, neither NiV nor LayV V proteins nor the mCh-V_{CTD} constructs inhibited
265 the activation of the IFN-β promoter after RIG-I stimulation (Figure 4C, D).
266 Overall, these results indicate that both NiV and LayV V can inhibit the IFN-β induction
267 pathway after the activation of MDA5 but not RIG-I.
268
269 ***The W protein of NiV, but not LayV, inhibits MDA5 and RIG-I signalling pathways***
270 When V proteins were replaced with W in the MDA5 and RIG-I activation assays, NiV W was
271 able to inhibit the activation of the IFN-β promoter upon both MDA5 (Figure 5A) and RIG-I
272 (Figure 5C) activation. This effect was stronger when only the CTD of NiV W protein was
273 expressed (mCh-W_{CTD}) (Figure 5B, D). Conversely, LayV W protein did not have any
274 inhibitory effect on the activation of the IFN-β promoter upon MDA5 and RIG-I activation
275 (Figure 5). To compensate for the lower expression of LayV W compared to NiV W (Figure

276 S2C), we transfected a range of plasmid quantities. While we detected an inverse correlation
277 between the amount of NiV W and the reporter signal intensity, the activation of the reporter's
278 promoter was insensitive to the increasing amount of LayV W, even when expressed at higher
279 levels than NiV W, thus indicating that the difference in inhibitory effect is protein-specific and
280 not due to the protein expression levels (Figure S3). This is further confirmed with the mCh-
281 W_{CTD} constructs, which are similarly expressed, with only NiV W_{CTD} being able to inhibit the
282 induction (Figure 5B, D, S2C).

283 While LayV W is found in the cytoplasm, NiV W is concentrated in the nucleus thanks
284 to an NLS present on W_{CTD} (Figure 1B, S1D). Since this signal is required for NiV W inhibitory
285 activity of immune pathways [37,43], we examined whether the absence of inhibitory activity
286 of LayV W would be due to its cytoplasmic localisation. Mutating NiV W NLS (NLSko)
287 relocated the mCh-W_{CTD} fusion protein in the cytoplasm, and adding back the exogenous NLS
288 of the simian vacuolating virus 40 ($SV40_{NLS}$) partially restored the nuclear localisation (Figure
289 6A). As expected, the inhibitory effect of these NiV mCh-W_{CTD} constructs on the IFN-β
290 promoter correlated with their intracellular localisation (Figure 6A, B). On the contrary, while
291 the addition of the $SV40_{NLS}$ to LayV mCh-W_{CTD} also partially relocated the protein to the
292 nucleus, this relocalisation did not provide any significant inhibitory effect to LayV W_{CTD}
293 (Figure 6A, C). Thus, the absence of an inhibitory effect of LayV W is not solely due to its
294 cytoplasmic localisation.

295

296 ***The NF-κB pathway and the translocation of p65 into the nucleus are impaired by NiV but***
297 ***not LayV W protein***

298 We have previously demonstrated that NiV W can inhibit the NF-κB pathway via its CTD [37].
299 Here, we analysed the effect of LayV and NiV proteins on the NF-κB pathway after stimulation
300 of cells with IL-1β (Figure 7A, B). Although weakly for the full-length proteins, the expression

301 of NiV W and W_{CTD} decreased the activation of the NF-κB promoter, while LayV proteins did
302 not and even increased the activity (Figure 7A, B).
303 Since NiV W decreases the nuclear concentration of NF-κB p65 subunit in infected
304 cells, we monitor the localisation of p65 after NiV or LayV W expression and IL-1β stimulation
305 (Figure 7C, D). While NiV W decreased the concentration of p65 in the nucleus via its CTD,
306 LayV W did not prevent the relocalisation of p65 in the nucleus upon IL-1β stimulation. These
307 results suggest that, unlike NiV W, LayV W is not able to inhibit the accumulation of p65 in
308 the nucleus and thus the subsequent activation of the NF-κB promoter.
309
310
311 **DISCUSSION**
312 The presence of the entry receptor(s) and the ability to counteract the host defence are among
313 the most important barriers for a virus to successfully infect a new host. For paramyxoviruses,
314 the proteins translated from the P gene (P, V, W, and C) are the main anti-host defence factors.
315 In the absence of a reverse genetic system for Langya virus, we used cell transfection assays to
316 assess the ability of LayV P, V, and W proteins to block several pathways of the intrinsic
317 immunity in human cells and compared them to NiV proteins, a closely related, zoonotic, and
318 highly pathogenic virus.
319 We report that both LayV and NiV V proteins can efficiently inhibit transcription
320 activation after MDA5 stimulation. Since the amino acids essential for the folding of the V_{CTD}
321 and the binding to MDA5 are highly conserved between NiV and LayV, and among henipa-
322 and parahenipaviruses (Figure S1C), LayV V likely directly binds to and blocks the activation
323 of MDA5. Although NiV V was described to decrease RIG-I activation via the inhibition of the
324 TRIM25-mediated ubiquitination of RIG-I [48], we did not observe any effect in our assays.
325 This discrepancy likely reflects differences in the assays, mainly the absence of overexpression

326 of TRIM25 and the use of different cell lines (HEK293T vs Huh-7.5). Thus, we cannot conclude
327 on the effect of LayV V on the TRIM25-mediated ubiquitination of RIG-I.

328 Similarly, LayV P can inhibit the signalling under the IFN-I receptor, but less efficiently
329 than NiV P. This difference does not seem correlated with P expression levels and may reflect
330 differences in their ability to bind human STAT proteins, as suggested by the rather low
331 conservation of the STAT1-binding region of NiV P.

332 Unlike NiV W, LayV W was unable to inhibit transcription activation after activation
333 of MDA5, RIG-I, and the IL-1β receptor. Since the transcription factor NF-κB is activated by
334 each of these signalling pathways, and is known to be inhibited by NiV W, NiV W may inhibit
335 these three pathways using the same molecular mechanism: recruiting the cellular protein 14-
336 3-3 to the nucleus to favour the export of p65 [37,49]. The relocation of LayV W to the nucleus,
337 where NiV W is concentrated, did not provide any functional effect, and LayV W lacks the
338 residues of NiV W known to bind 14-3-3. Thus, unlike NiV W, LayV W is most likely not able
339 to recruit 14-3-3 to the nucleus to inhibit p65 accumulation.

340 Since the C protein also participates in the immune evasion, and LayV is thought to
341 express an additional protein upstream of the F open reading frame (Figure 1B), these two
342 proteins may contribute to the immune evasion and compensate for the absence of activity of
343 LayV W in inhibiting the human immunity pathways.

344 Overall, this study suggests that the P and W proteins of LayV are not as efficient as
345 NiV proteins in counteracting human intrinsic immunity. Thus, since the inhibition of the innate
346 immune system is a major factor of pathogenicity, this distinction between NiV and LayV may
347 be one of the reasons for the difference in pathogenicity observed in humans, with the high
348 lethality of NiV-infected patients, in contrast to LayV infection.

349

ACKNOWLEDGEMENTS

We acknowledge the contribution of the SFR Biosciences (Université Claude Bernard Lyon 1, CNRS UAR3444, Inserm US8, ENS de Lyon) LYMIC-PLATIM microscopy platform for training and the use of the LSM800 AS confocal microscope. We thank Mathieu Iampietro and Lucia Amurri (CIRI, Lyon) for their advice on the NF-κB experiments and all current and former members of the team Immunobiology of Viral Infections at CIRI for their help in the realisation of the study. We thank Omran Allatif (CIRI, bioinformatics and biostatistics (BIBS) platform) for his help with statistical analysis.

FUNDING STATEMENT

The work was supported by the Institut National de la Santé et de la Recherche Médicale (Inserm), the Centre National de la Recherche Scientifique (CNRS), the Aviesan Sino-French agreement on Nipah virus study, and is part of the "Investissements d'Avenir ExcellencES" program from the French National Research Agency (Shape-Med@Lyon; ANR-22-EXES-0012).

DISCLOSURE STATEMENT

The authors report no conflict of interest.

DATA AVAILABILITY STATEMENT

Data is available upon request.

371 **REFERENCES**

372 [1] Zhang X-A, Li H, Jiang F-C, et al. A Zoonotic Henipavirus in Febrile Patients in
373 China. N Engl J Med. 2022;387(5):470–472.

374 [2] Natasha A, Pye SE, Park K, et al. Detection and characterization of Langya virus in
375 *Crocidura lasiura* , Republic of Korea [Internet]. 2024 [cited 2024 Dec 17]. Available
376 from: http://biorxiv.org/lookup/doi/10.1101/2024.12.02.626520.

377 [3] Parry RH, Yamada KYH, Hood WR, et al. Henipavirus in Northern Short-Tailed
378 Shrew, Alabama, USA. Emerg Infect Dis. 2025;31(2):392–394.

379 [4] Zhang J-T, Hu Z-Y, Tang F, et al. Decoding the RNA viromes in shrew lungs along the
380 eastern coast of China. NPJ Biofilms Microbiomes. 2024;10(1):68.

381 [5] Wu Z, Yang L, Yang F, et al. Novel Henipa-like virus, Mojiang Paramyxovirus, in rats,
382 China, 2012. Emerg Infect Dis. 2014;20(6):1064–1066.

383 [6] Lee S-H, Kim K, Kim J, et al. Discovery and Genetic Characterization of Novel
384 Paramyxoviruses Related to the Genus Henipavirus in Crocidura Species in the
385 Republic of Korea. Viruses. 2021;13(10):2020.

386 [7] Vanmechelen B, Meurs S, Horemans M, et al. The characterization of multiple novel
387 paramyxoviruses highlights the diverse nature of the subfamily Orthoparamyxovirinae.
388 Virus Evol. 2022;8(2):veac061.

389 [8] Horemans M, Van Bets J, Joly Maes T, et al. Discovery and genome characterization
390 of six new orthoparamyxoviruses in small Belgian mammals. Virus Evol.
391 2023;9(2):vead065.

392 [9] Chen Y-M, Hu S-J, Lin X-D, et al. Host traits shape virome composition and virus
393 transmission in wild small mammals. Cell. 2023;186(21):4662-4675.e12.

394 [10] Haring VC, Litz B, Jacob J, et al. Detection of novel orthoparamyxoviruses,
395 orthonairoviruses and an orthohepevirus in European white-toothed shrews. Microb
396 Genomics. 2024;10(8):001275.

397 [11] Vanmechelen B, Balkema-Buschmann A, Drexler F, et al. Taxonomic reorganization of
398 the family Paramyxoviridae [Internet]. 2023. Available from:
399 https://www.google.com/url?sa=t&source=web&rct=j&opi=89978449&url=https://ictv
400 .global/system/files/proposals/approved/Animal_dsRNA_and_ssRNA-
401 _viruses/2023.018M.Paramyxoviridae_reorg.docx&ved=2ahUKEwjVq8SBiZ6OAxVIc
402 KQEHTWZE9cQFnoECD4QAQ&usg=AOvVaw0lkIr3W06nbxmNzrDMife-.

403 [12] Byrne PO, Blade EG, Fisher BE, et al. Prefusion stabilization of the Hendra and
404 Langya virus F proteins. J Virol. 2024;98(2):e0137223.

405 [13] Guo Y, Wu S, Li W, et al. The cryo-EM structure of homotetrameric attachment
406 glycoprotein from langya henipavirus. Nat Commun. 2024;15(1):812.

407 [14] Isaacs A, Low YS, Macauslane KL, et al. Structure and antigenicity of divergent
408 Henipavirus fusion glycoproteins. Nat Commun. 2023;14(1):3577.

[15] May AJ, Pothula KR, Janowska K, et al. Structures of Langya Virus Fusion Protein Ectodomain in Pre- and Postfusion Conformation. J Virol. 2023;97(6):e0043323.

[16] Wang C, Li M, Wang Y, et al. Structural insights into the Langya virus attachment glycoprotein. Struct Lond Engl 1993. 2024;32(8):1090-1098.e3.

[17] Wang Z, McCallum M, Yan L, et al. Structure and design of Langya virus glycoprotein antigens. Proc Natl Acad Sci U S A. 2024;121(16):e2314990121.

[18] Pelissier R, Iampietro M, Horvat B. Recent advances in the understanding of Nipah virus immunopathogenesis and anti-viral approaches. F1000Research. 2019;8.

[19] Mehand MS, Al-Shorbaji F, Millett P, et al. The WHO R&D Blueprint: 2018 review of emerging infectious diseases requiring urgent research and development efforts. Antiviral Res. 2018;159:63–67.

[20] Lo MK, Harcourt BH, Mungall BA, et al. Determination of the henipavirus phosphoprotein gene mRNA editing frequencies and detection of the C, V and W proteins of Nipah virus in virus-infected cells. J Gen Virol. 2009;90(Pt 2):398–404.

[21] Fontana JM, Bankamp B, Rota PA. Inhibition of interferon induction and signaling by paramyxoviruses. Immunol Rev. 2008;225(1):46–67.

[22] Pelissier R, Iampietro M, Horvat B. Recent advances in the understanding of Nipah virus immunopathogenesis and anti-viral approaches. F1000Research. 2019;8.

[23] Mathieu C, Guillaume V, Volchkova VA, et al. Nonstructural Nipah virus C protein regulates both the early host proinflammatory response and viral virulence. J Virol. 2012;86(19):10766–10775.

[24] Satterfield BA, Cross RW, Fenton KA, et al. The immunomodulating V and W proteins of Nipah virus determine disease course. Nat Commun. 2015;6:7483.

[25] Satterfield BA, Cross RW, Fenton KA, et al. Nipah Virus C and W Proteins Contribute to Respiratory Disease in Ferrets. J Virol. 2016;90(14):6326–6343.

[26] Satterfield BA, Borisevich V, Foster SL, et al. Antagonism of STAT1 by Nipah virus P gene products modulates disease course but not lethal outcome in the ferret model. Sci Rep. 2019;9(1):16710.

[27] Rodriguez JJ, Parisien J-P, Horvath CM. Nipah Virus V Protein Evades Alpha and Gamma Interferons by Preventing STAT1 and STAT2 Activation and Nuclear Accumulation. J Virol. 2002;76(22):11476–11483.

[28] Park M-S, Shaw ML, Muñoz-Jordan J, et al. Newcastle disease virus (NDV)-based assay demonstrates interferon-antagonist activity for the NDV V protein and the Nipah virus V, W, and C proteins. J Virol. 2003;77(2):1501–1511.

[29] Shaw ML, García-Sastre A, Palese P, et al. Nipah Virus V and W Proteins Have a Common STAT1-Binding Domain yet Inhibit STAT1 Activation from the Cytoplasmic and Nuclear Compartments, Respectively. J Virol. 2004;78(11):5633–5641.

446 [30] Rodriguez JJ, Cruz CD, Horvath CM. Identification of the nuclear export signal and
447 STAT-binding domains of the Nipah virus V protein reveals mechanisms underlying
448 interferon evasion. J Virol. 2004;78(10):5358–5367.

449 [31] Ciancanelli MJ, Volchkova VA, Shaw ML, et al. Nipah virus sequesters inactive
450 STAT1 in the nucleus via a P gene-encoded mechanism. J Virol. 2009;83(16):7828–
451 7841.

452 [32] Jensen MR, Yabukarski F, Communie G, et al. Structural Description of the Nipah
453 Virus Phosphoprotein and Its Interaction with STAT1. Biophys J. 2020;118(10):2470–
454 2488.

455 [33] Keiffer TR, Ciancanelli MJ, Edwards MR, et al. Interactions of the Nipah Virus P, V,
456 and W Proteins across the STAT Family of Transcription Factors. mSphere. 2020;5(6).

457 [34] Andrejeva J, Childs KS, Young DF, et al. The V proteins of paramyxoviruses bind the
458 IFN-inducible RNA helicase, mda-5, and inhibit its activation of the IFN-β promoter.
459 Proc Natl Acad Sci U S A. 2004;101(49):17264–17269.

460 [35] Childs K, Stock N, Ross C, et al. mda-5, but not RIG-I, is a common target for
461 paramyxovirus V proteins. Virology. 2007;359(1):190–200.

462 [36] Wagner ND, Liu H, Rohrs HW, et al. Nipah Virus V Protein Binding Alters MDA5
463 Helicase Folding Dynamics. ACS Infect Dis. 2022;8(1):118–128.

464 [37] Enchéry F, Dumont C, Iampietro M, et al. Nipah virus W protein harnesses nuclear 14-
465 3-3 to inhibit NF-κB-induced proinflammatory response. Commun Biol.
466 2021;4(1):1292.

467 [38] Louber J, Brunel J, Uchikawa E, et al. Kinetic discrimination of self/non-self RNA by
468 the ATPase activity of RIG-I and MDA5. BMC Biol. 2015;13:54.

469 [39] King P, Goodbourn S. The beta-interferon promoter responds to priming through
470 multiple independent regulatory elements. J Biol Chem. 1994;269(48):30609–30615.

471 [40] Kuri P, Ellwanger K, Kufer TA, et al. A high-sensitivity bi-directional reporter to
472 monitor NF-κB activity in cell culture and zebrafish in real time. J Cell Sci.
473 2017;130(3):648–657.

474 [41] Louber J, Kowalinski E, Bloyet L-M, et al. RIG-I Self-Oligomerization Is Either
475 Dispensable or Very Transient for Signal Transduction. Boudinot P, editor. PLoS ONE.
476 2014;9(9):e108770.

477 [42] Katoh K, Rozewicki J, Yamada KD. MAFFT online service: multiple sequence
478 alignment, interactive sequence choice and visualization. Brief Bioinform.
479 2019;20(4):1160–1166.

480 [43] Shaw ML, Cardenas WB, Zamarin D, et al. Nuclear localization of the Nipah virus W
481 protein allows for inhibition of both virus- and toll-like receptor 3-triggered signaling
482 pathways. J Virol. 2005;79(10):6078–6088.

483 [44] Lo MK, Harcourt BH, Mungall BA, et al. Determination of the henipavirus
484 phosphoprotein gene mRNA editing frequencies and detection of the C, V and W
485 proteins of Nipah virus in virus-infected cells. J Gen Virol. 2009;90(2):398–404.

486 [45] Smith KM, Tsimbalyuk S, Edwards MR, et al. Structural basis for importin alpha 3
487 specificity of W proteins in Hendra and Nipah viruses. Nat Commun. 2018;9(1):3703.

488 [46] Motz C, Schuhmann KM, Kirchhofer A, et al. Paramyxovirus V Proteins Disrupt the
489 Fold of the RNA Sensor MDA5 to Inhibit Antiviral Signaling. Science.
490 2013;339(6120):690–693.

491 [47] Ramachandran A, Horvath CM. Dissociation of Paramyxovirus Interferon Evasion
492 Activities: Universal and Virus-Specific Requirements for Conserved V Protein Amino
493 Acids in MDA5 Interference. J Virol. 2010;84(21):11152–11163.

494 [48] Sánchez-Aparicio MT, Feinman LJ, García-Sastre A, et al. Paramyxovirus V Proteins
495 Interact with the RIG-I/TRIM25 Regulatory Complex and Inhibit RIG-I Signaling. J
496 Virol. 2018;92(6):e01960-17.

497 [49] Edwards MR, Hoad M, Tsimbalyuk S, et al. Henipavirus W Proteins Interact with 14-
498 3-3 To Modulate Host Gene Expression. J Virol. 2020;94(14):e00373-20.

499

500 **FIGURES**

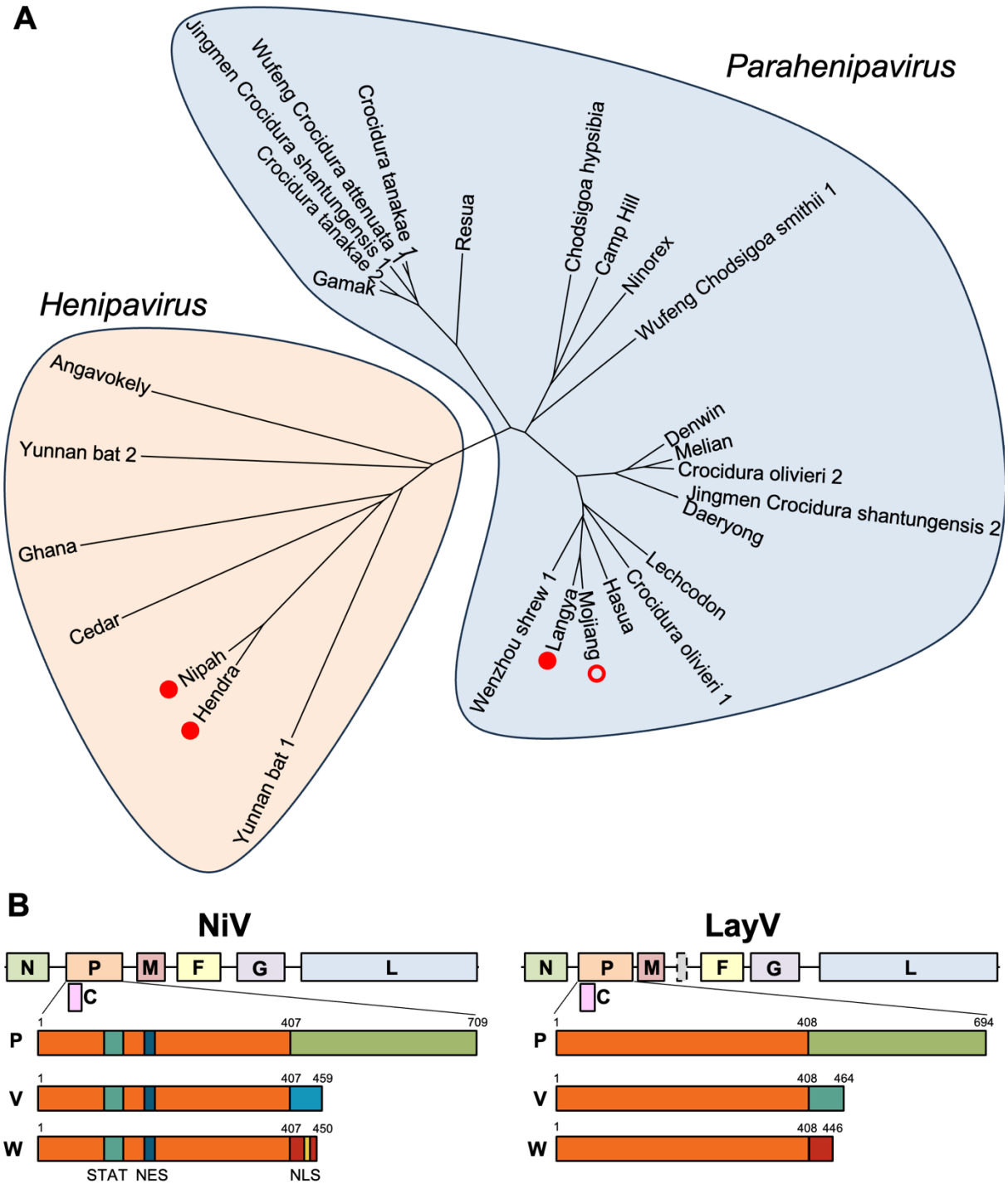

501

502 ***Figure 1. Phylogenetic tree and genome organisation of henipaviruses and***

503 ***parahenipaviruses.***

504 (A) Phylogenetic tree of henipavirus and parahenipaviruses based on the protein sequence of

505 the L protein. Red dots indicate viruses known to be pathogenic in humans, and the red circle

506 indicates Mojiang virus, suspected to be pathogenic for humans [5]. (B) Genome organisation
507 of NiV and LayV. The proteins produced from the P gene are indicated below the genomes. A
508 STAT1-binding site (STAT), a nucleus export signal (NES), and a nucleus localisation signal
509 (NLS), described for NiV, are indicated.

510 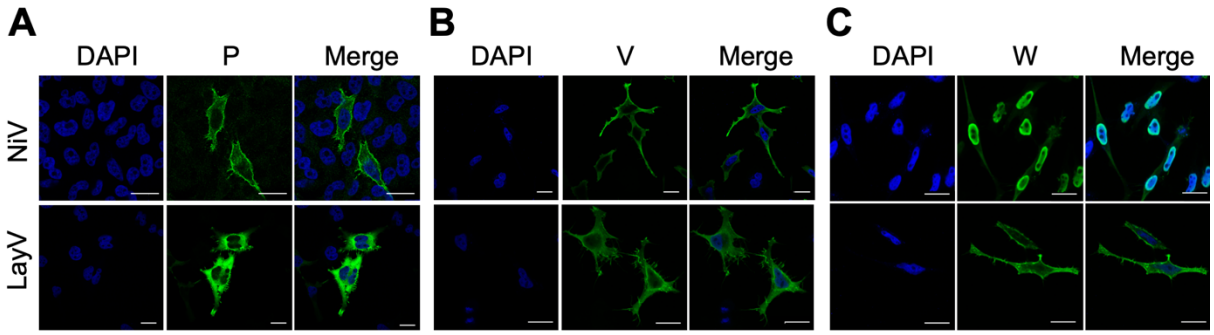

511 ***Figure 2. Localisation of NiV and LayV P, V, and W proteins.***

512 HeLa cells were transfected to express NiV or LayV Flag-tagged P (A), V (B), or W (C). At 24

513 h.p.t., proteins were stained using an anti-Flag antibody and imaged by confocal microscopy.

514 Viral proteins are in green, and nuclei are in blue. Scale bars correspond to 20 µm.

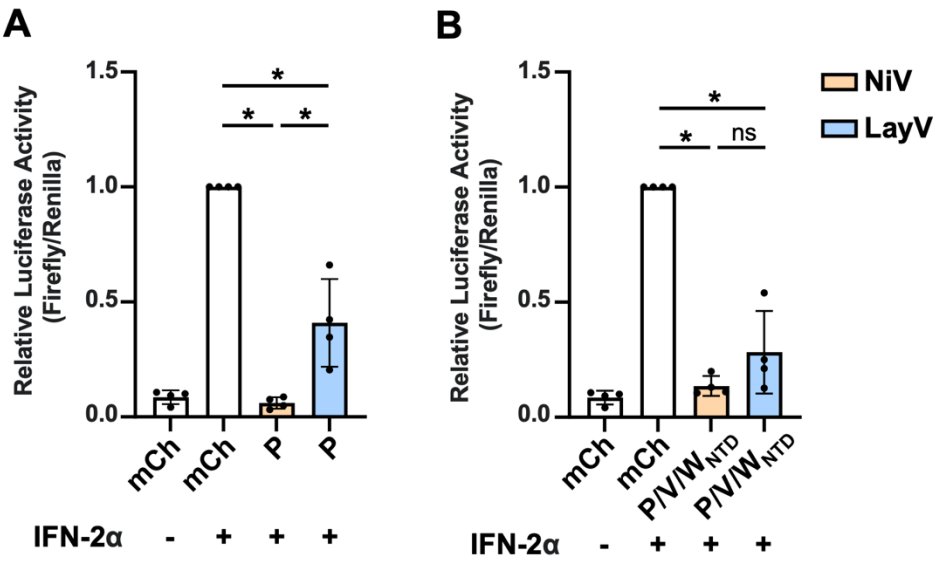

515

516 ***Figure 3. NiV and LayV P/V/W$_{NTD}$ inhibit the IFN-I signalling pathway.***

517 HEK293T cells were co-transfected with three plasmids coding for (1) a viral protein or the
518 mCherry (mCh) control, (2) the Firefly luciferase under an ISRE-dependent promoter, and (3)
519 the Renilla luciferase under a constitutive promoter. Either the full-length P proteins are
520 expressed (A) or only the N-terminal domain common to P, V, and W (P/V/W$_{NTD}$) (B). At 18
521 h.p.t., cells were stimulated with 1000 U/mL IFN-2α for 24 h before measuring the luciferase
522 activities. Mean and SD were calculated from four independent experiments.

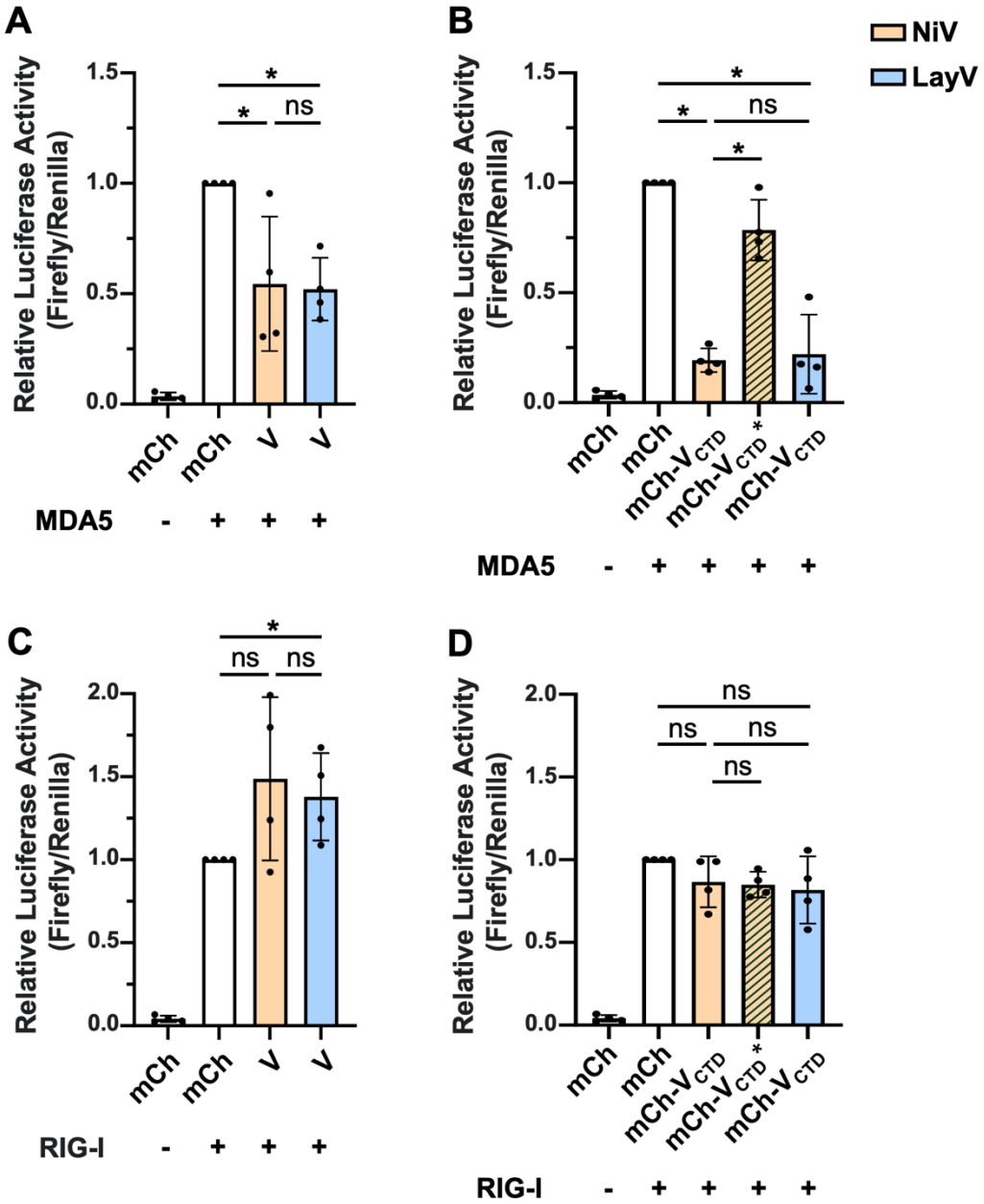

523

524 ***Figure 4. NiV and LayV V proteins inhibit MDA5 but not RIG-I signalling pathway.***

525 Huh-7.5 cells were co-transfected with four plasmids coding for (1) human MDA5 (A, B) or
526 RIG-I (C, D), (2) a viral protein or the mCherry control, (3) the Firefly luciferase under the
527 IFN-β promoter, and (4) the Renilla luciferase under a constitutive promoter. Viral proteins are
528 expressed either as full-length proteins (A, C) or as fusion proteins between mCherry and the
529 V C-terminal domain (mCh-V_{CTD}) (B, D). Cells were stimulated 24 h.p.t. by transfecting 100
530 ng Poly(I:C), and the luciferase activities were measured 48 h.p.t. Mean and SD were calculated
531 from four independent experiments. mCh-V_{CTD}* carries the mutations E411A and I414A.

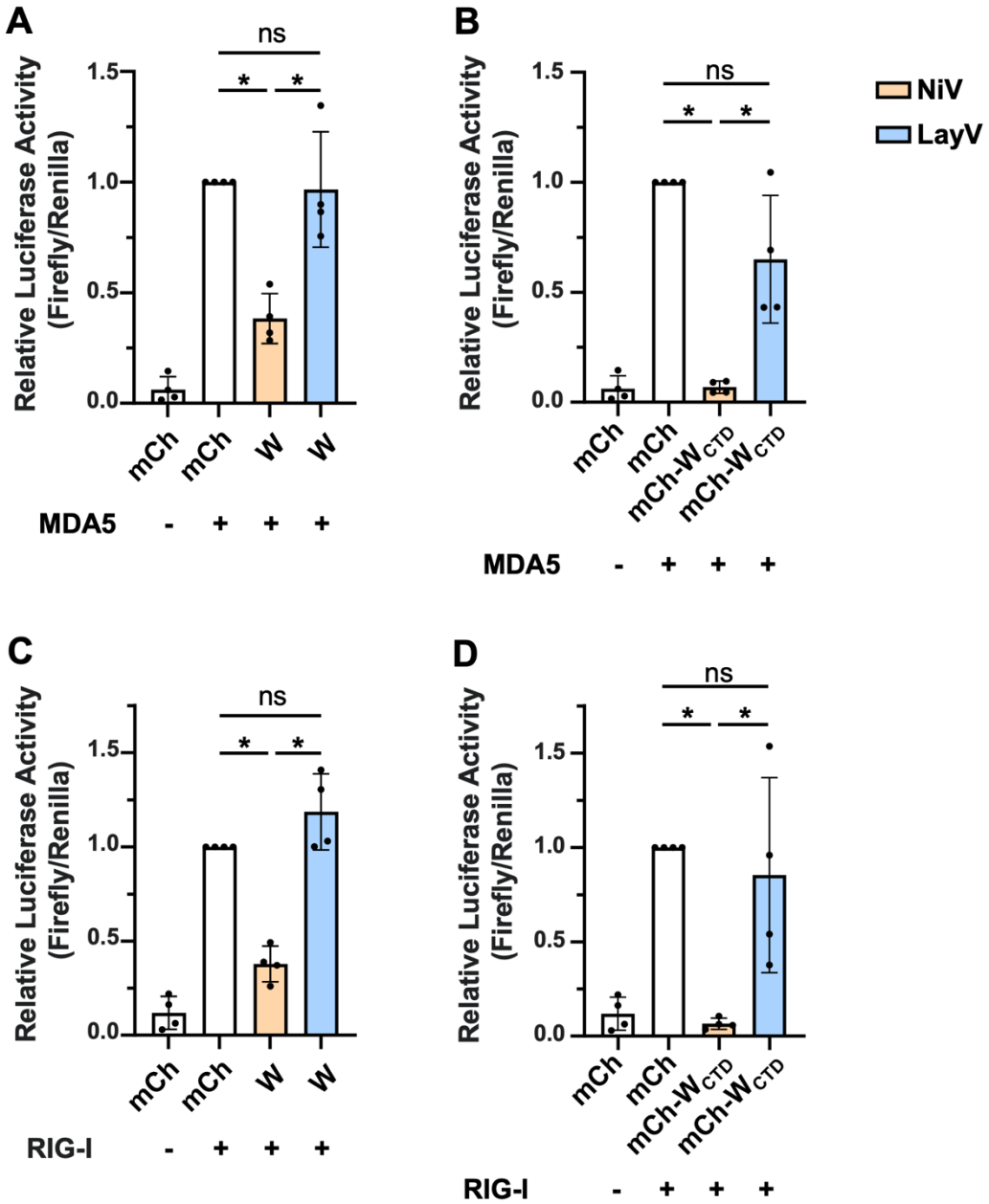

532

533 ***Figure 5. Only NiV W protein inhibits MDA5 and RIG-I signalling pathways.***

534 Huh-7.5 cells were co-transfected with four plasmids coding for (1) human MDA5 (A, B) or
535 RIG-I (C, D), (2) a viral protein, (3) the Firefly luciferase under the IFN-β promoter, and (4)
536 the Renilla luciferase under a constitutive promoter. Viral proteins are expressed either as full-
537 length proteins (A, C) or as fusion proteins between mCherry and the W C-terminal domain
538 (mCh-W_{CTD}) (B, D). Cells were stimulated 24 h.p.t. by transfecting 100 ng of Poly(I:C), and
539 luciferase activities were measured 48 h.p.t. Mean and SD were calculated from four
540 independent experiments.

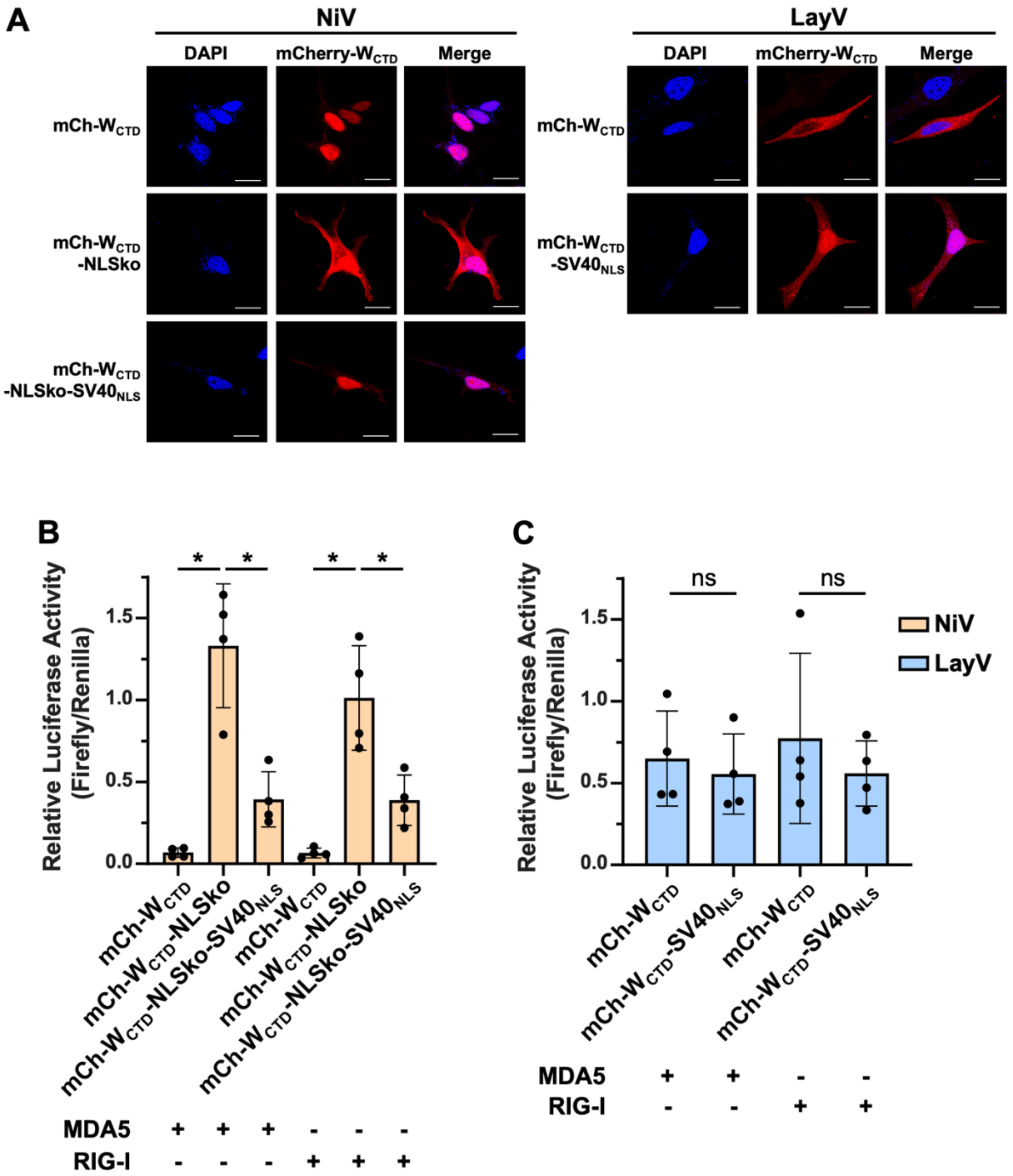

541

542 ***Figure 6. The cytoplasmic localisation of LayV W is not responsible for the absence of***

543 ***inhibition of the MDA5 and RIG-I pathways.***

544 (A) HeLa cells were transfected to express fusion proteins between mCherry and NiV or LayV

545 W C-terminal domain (mCh-W_{CTD}). In some constructs, the nuclear localisation signal (NLS)

546 of NiV W was mutated (NLSko), and the NLS from SV40 was added to NiV and LayV W_{CTD}

547 ($SV40_{NLS}$). Twenty-four hours post-transfection, stained cells were imaged by confocal

548 microscopy. Viral proteins are in red and nuclei in blue. Scale bars correspond to 20 µm. (B,
549 C) Huh-7.5 cells were co-transfected with four plasmids coding for (1) human MDA5 or RIG-
550 I, (2) a viral protein or the mCherry control, (3) the Firefly luciferase under the IFN-β promoter,
551 and (4) the Renilla luciferase under a constitutive promoter. Cells were stimulated 24 h.p.t. by
552 transfecting 100 ng of Poly(I:C), and relative activities of the luciferases were measured 48
553 h.p.t. Mean and SD were calculated from four independent experiments.

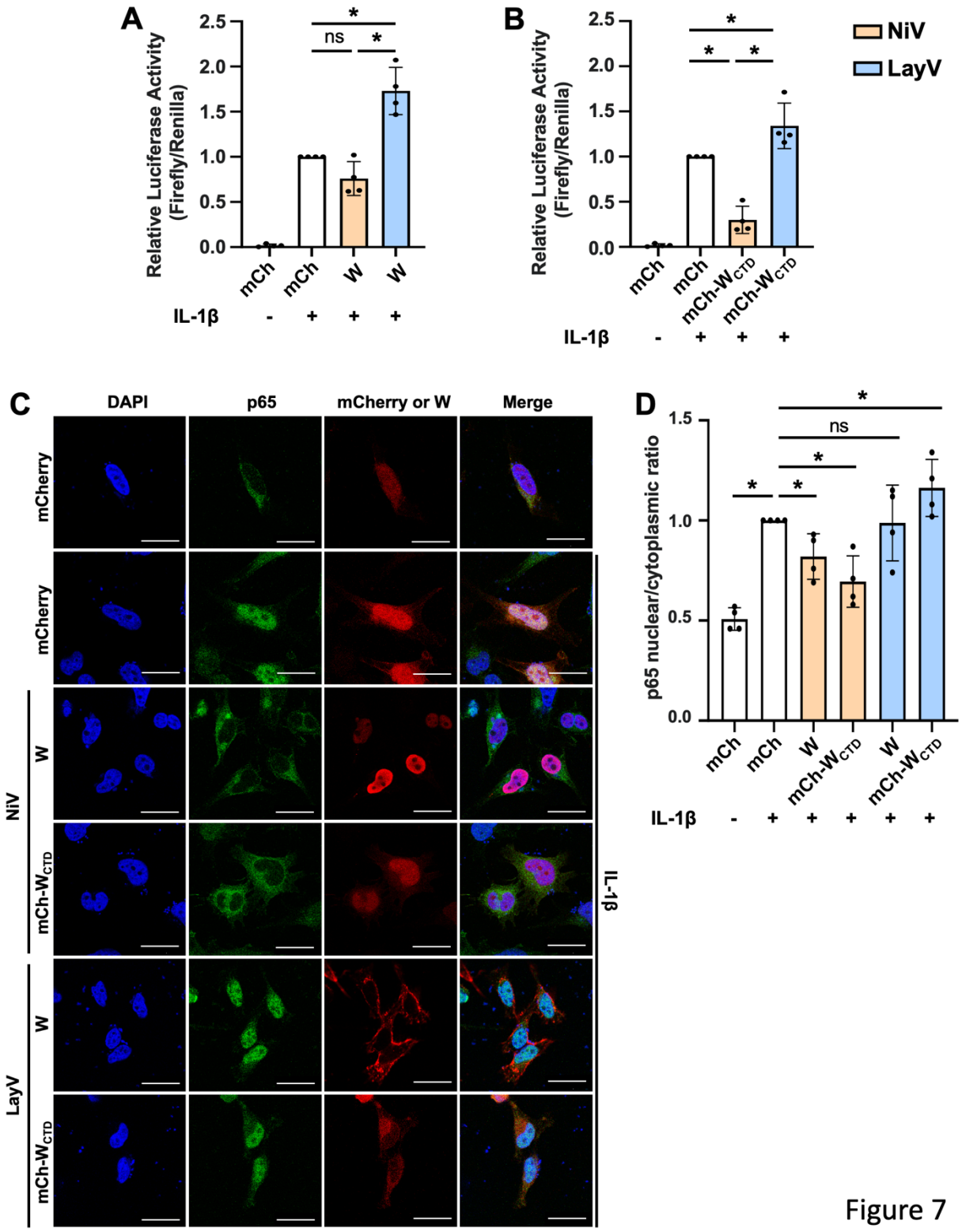

Figure 7. NiV but not LayV W protein can block the NF-κB pathway.

(A and B) HeLa cells were co-transfected with three plasmids coding for (1) a viral protein or the mCherry control, (2) the Firefly luciferase under an NF-κB-dependent promoter, and (3) the Renilla luciferase under a constitutive promoter. Viral proteins are expressed either as full-

559 length proteins (A) or as fusion proteins between mCherry and the W C-terminal domain (mCh-
560 W_{CTD}) (B). At 18 h.p.t., cells were incubated with 10 ng/mL IL-1β for 2 h before measuring the
561 luciferase activities. Mean and SD were calculated from four independent experiments. (C)
562 HeLa cells were transfected to express NiV or LayV W or mCh-W_{CTD} viral proteins. At 24
563 h.p.t., cells were stimulated with 10 ng/mL IL-1β for 20 min before being fixed. W was stained
564 with an anti-Flag antibody and endogenous p65 protein with an anti-NF-κB p65 antibody.
565 Stained cells were imaged by confocal microscopy. Nuclei are in blue, p65 in green, and viral
566 proteins in red. Scale bars correspond to 20 µm. (D) The mean intensity of nuclear and
567 cytoplasmic NF-κB p65 was evaluated using QuPath software on an average of 150 events per
568 condition. Mean and SD were calculated from four independent experiments.